ASSESSMENT OF FISSION GAS RELEASE BEHAVIOUR IN UO_2 DOPED FUEL USING FEMAXI-6 CODE

DRAGOŞ VICTOR IONESCU, ALEXANDRU GABRIEL NUŢĂ, ALINA CRISTINA IVAŞCU

Institute for Nuclear Research (RATEN ICN) Pitești, Romania

e-mail: dragos.ionescu@nuclear.ro

Abstract

This study presents the implementation of a modified fission gas diffusion model in the FEMAXI-6 code for UO_2 doped fuel. The model introduces corrections to the effective diffusion coefficient in order to account for the influence of dopant-induced changes. The model was implemented in FEMAXI-6 and compared with two irradiation experiments operated under different power histories involving five fuel rods from which four with UO_2 doped fuel. Calculated maximum fuel temperature, rod internal pressure, and fission gas release were compared with experimental data. The model provides improved predictions of fission gas release compared to the standard FEMAXI-6 formulation. However, deviations are observed in high-release cases, suggesting that additional mechanisms such as grain boundary saturation and microstructural evolution should be included.

Keywords: *Fission gas release, FEMAXI-6, UO_2 doped fuel, Diffusion*

Introduction

Fission gas release (FGR) remains one of the most important phenomena in fuel rod performance analysis since it directly controls free-volume pressure, contributes to fuel swelling, reduces gap conductance when associated with bubble accumulation, and interacts with pellet cracking and pellet–cladding mechanical interaction [1-3]. In oxide fuels, the gas atoms generated by fission are initially retained within the grains, where they diffuse toward grain boundaries, form bubbles, and are eventually released to the rod free volume when grain-edge bubbles connectivity and grain-face interlinkage become sufficiently developed. The kinetics of that sequence is strongly nonlinear and depends on temperature, irradiation history, burnup, microstructure, and stress state [2-4].

Engineering fuel performance codes have historically described intragranular gas transport through a Booth-type diffusion treatment coupled with an effective diffusion coefficient, often derived from the classical work of Turnbull and co-workers [1, 5]. This approach remains robust and computationally convenient, but it necessarily compresses several processes into a single effective parameter. As a result, standard diffusivity correlations can reproduce average behaviour in many steady-state cases, but they often struggle when the fuel experiences strong transients, when the stress field evolves significantly, or when the microstructure departs from the standard fine-grained UO_2 condition [3-5].

The need for more mechanistic treatments has motivated the development of multi-component diffusivity models and transient release models in several modern fuel codes [3, 6, 7]. Among these developments, Cooper formulation is especially relevant because it provides a physically motivated correction to the diffusivity of doped UO_2 fuel and explicitly distinguishes how the different components of the effective diffusion coefficient are altered [8]. In the source model used here, the corrected diffusivity is formulated from the undoped basis by temperature-dependent exponential factors applied to the first two diffusional contributions, while the third contribution is retained. This structure is attractive for implementation in an engineering code because it preserves continuity with the standard Turnbull-style decomposition and can therefore be inserted without rewriting the entire gas behaviour framework.

The present paper describes the implementation of the Cooper [8] diffusion correction in FEMAXI-6 and its application to two irradiation campaigns represented by five fuel rods [9]. The analysis considers three coupled quantities: maximum fuel temperature, rod internal pressure and cumulative FGR, in order to separate the thermal, mechanical and gas transport effects. The results are used to assess the effect of the corrected diffusivity on the fuel behavior and to identify its limitations, as well as the need for additional mechanism such as grain-boundary saturation and burnup-driven microstructural evolution.

Theoretical basis of the implemented model

The generally accepted physical description of FGR in UO_2 is inherently multistage. Gas atoms such as xenon and krypton are produced in the fuel matrix, where they can remain dissolved for a while before migration by vacancy-assisted diffusion. Part of the gas is retained in intragranular bubbles, some reaches grain boundaries, and some is eventually released into the free volume once the grain-boundary bubble network becomes connected [2, 3].

Because the transport length is on the order of the grain radius, intragranular diffusion is highly sensitive to both temperature and grain size. In contrast, grain-boundary processes affect whether the gas that reaches the boundary remains trapped or rapidly released [2, 4, 6].

For a spherical grain of radius R, the classical Booth solution gives the fractional release as a function of the dimensionless group DT/R^2 [1]. The main implication is that any modification of the effective diffusivity D can have a large effect on release when the fuel operates in regimes where DT/R^2 changes from subcritical to dominant values. This explains why even relatively modest variations in the diffusion coefficient may lead to substantial differences in cumulative fission gas release over prolonged irradiation histories or under conditions involving power ramps [3, 6].

$$D_{eff} = D_1 + D_2 + D_3 \quad (1)$$

where D_1 is the thermally activated high-temperature component, D_2 is an irradiation-related contribution that depends on fission rate, and D_3 is athermal or low-temperature irradiation contribution [5]. The main advantage of this decomposition is that it retains compact algebra while still allowing the dominant dependencies on temperature and irradiation conditions to be identified explicitly.

The limitation of the standard framework is not conceptual but parametric. While the three-term formulation may adequately describe conventional fine-grained UO_2, its applicability is not necessarily preserved when dopants modify defect energetics, local stress fields affect vacancy transport, or irradiation-induced microstructural evolution departs from the conditions underlying the original calibration [3, 5, 8]. In such cases, the practical question is not whether the three-term structure should be discarded, but whether its coefficients be revised in a manner that preserves both physically meaningful and numerically stable. The Cooper correction addresses exactly to this need [8].

$$D^{doped} = C_1 \cdot D_1^{undoped} + C_2 \cdot D_2^{undoped} + D_3^{undoped} \quad (2)$$

where $C_1 = e^{\frac{H_1}{k_b}\left(\frac{1}{T}-\frac{1}{T_1}\right)}$, $C_2 = e^{\frac{H_2}{k_b}\left(\frac{1}{T}-\frac{1}{T_2}\right)}$, k_b is the Boltzmann constant, T is the local fuel temperature, and $D_1^{undoped}$, $D_2^{undoped}$ and $D_3^{undoped}$ are the three contributions of the standard undoped-fuel diffusivity [8].

In the present implementation, case A of the Cooper model was selected, in accordance with the user requirement and the source article. For this case, the parameters are $T_1 = T_2 = 1773$ K, $\Delta H_1 = 0.3198$ eV and $\Delta H_2 = -0.3345$ eV [8]. The positive and negative values of ΔH_1 and ΔH_2 indicate that the correction does not follow a uniform multiplicative scale, but rather changes the relative weights of the first two contributions based on temperature.

The correction structure is physically significant because it preserves the standard low-temperature term D_3, ensuring consistency with the undoped reference model in the irradiation-dominated regime. At the same time, it allows for distinct modifications of the thermally activated and irradiation-coupled high-temperature terms. This reflects the physical expectation that dopants do not merely rescale the overall diffusivity, but instead alter defect formation and migration energetics in a mechanism- and temperature-dependent manner [8].

The Cooper-corrected diffusivity is implemented within FEMAXI-6, which already solves the coupled thermo-mechanical behaviour of the fuel rod. Consequently, although the correction is formulated mainly as a temperature-dependent modification of the undoped diffusivity, its effect is not exclusively thermal. The local fuel temperature depends on the power history, thermal conductivity degradation, cracking, fuel-clad gap evolution and contact conditions, all of which are computed by FEMAXI-6 [10]. Likewise, internal pressure depends on the amount of released gas and on the free volume history.

Within this coupled framework, the corrected diffusivity influences not only fission gas release, but also pressure development and, through feedback effects, the rod thermal state. This has important implications for how results are interpreted. A discrepancy between measured and calculated FGR cannot be attributed exclusively to diffusivity error; it may also reflect limitations in the grain-boundary release model, incomplete representation of segment-specific thermal conditions, or insufficient consideration of microstructural evolution. For this reason, the present assessment is based on three coupled observables: temperature, pressure, and gas release, rather than FGR alone. This multi-observable approach is consistent with current best practices for fuel performance assessment [3, 6, 7].

Implementation in FEMAXI-6

FEMAXI-6 is a well-established fuel rod behaviour code, developed for analyzing the thermal and mechanical response of oxide fuel rods under steady-state and transient conditions [10]. In the baseline model, fission gas release is described by intragranular diffusion coupled with semi-empirical models for gas transfer to the grain boundaries and subsequent release to the free volume. In the present work, a deliberately conservative implementation strategy was adopted: the corrected diffusivity was introduced into the existing FGR framework without modification of unrelated sub-models. This approach enabled the specific effect of the Cooper correction to be isolated.

In practical terms, at each time step, the code evaluates the local thermal state, computes the standard undoped diffusivity components D_1, D_2 and D_3, and replaces the effective coefficient used in the FGR routine with the Cooper case A corrected value. Since the correction is expressed directly in terms of the undoped components, the modification can be introduced at a single well-defined point in the diffusivity calculation chain. The rest of the gas release algorithm is left unchanged. This reduces the possibility that the observed differences originate from unrelated implementation modifications.

Experimental data and analysis methodology

The experimental data consists of two irradiation campaigns from the Halden Reactor Project: IFA-677 and IFA-716, [9]. The analysis includes three fuel rods from IFA-677 (rods 1, 5, and 6) and two fuel rods from IFA-716 (rods 1 and 6). Together, these campaigns provide a useful contrast in operating history and gas release behaviour. IFA-677 is characterized by higher linear power, repeated shutdowns or sharp power reductions, and a pronounced late increase in cumulative FGR, whereas IFA-716 exhibits lower power, longer irradiation duration, and lower gas release. As shown in Figure 1, the rods within each campaign follow closely similar power histories, with IFA-677 operating mostly between about 30 and 45 kW/m and IFA-716 between about 24 and 31 kW/m. This similarity within each series is methodologically beneficial as it reduces the influence of large differences in external operating conditions and allows the assessment to focus more directly on the model's ability to reproduce different measured gas release responses under otherwise comparable irradiation histories.

Taking into consideration that the analyzed rods are segmented, the assessment was performed at the segment level to preserve the physical correspondence between axial power history, measured temperature, and estimated response. For IFA-677, results were reported for segment 2 as well as for segments 1 and 3 combined, whereas IFA-716 consisted of two individual segments. Accordingly, FEMAXI-6 was applied in a manner that retained segment-specific thermal behaviour, and these outputs were used directly in the comparison. Methodologically, the implementation also offers a distinct advantage: since only the diffusivity term was modified, the comparison isolates the specific contribution of the Cooper correction within an engineering code framework already familiar to the fuel performance community. The present work should therefore be regarded not as a broad code-development effort, but as a targeted model implementation study focused on improving the intragranular fission gas diffusion coefficient.

The maximum fuel temperature, rod internal pressure, and cumulative FGR were all compared between calculated and measured values. Temperature is used to verify that the thermal field driving the diffusion model is realistic. While the internal pressure served as an integrated indicator of total gas release and free-volume evolution, FGR was taken as the primary observable of gas behaviour.

Since the available figures [9-11] do not provide raw numerical data, the final FGR values described later were estimated approximately from the endpoints of the published curves. These estimates are suitable for engineering interpretation and comparative assessment of model performance, but they should be regarded as graphical approximations rather than re-digitized benchmark data.

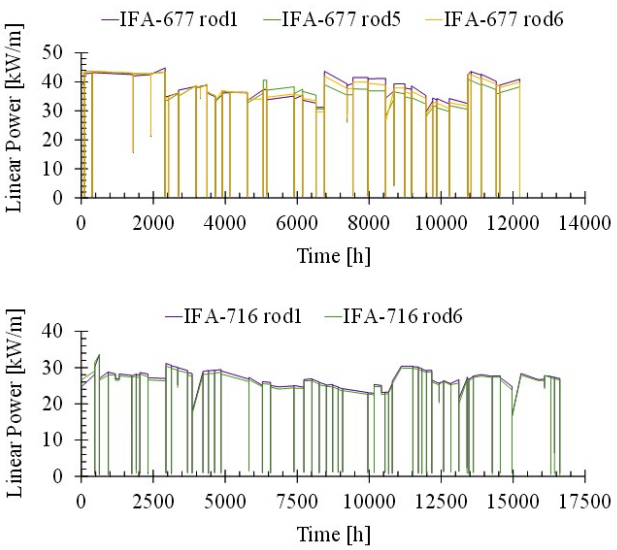


Fig. 1. Linear power histories used for IFA-677 (top) and IFA-716 (bottom)

Results

This section discusses the results rod by rod, for each experiment. For each case, the emphasis is on how well the model reproduces the evolution of temperature, pressure and FGR, and on what the deviations reveal about the adequacy and limitations of the corrected diffusivity.

Experiment IFA-677Rod1

IFA-677Rod1 is the most demanding case of Experiment 1 because it combines a comparatively high-power level with a strong late increase of measured FGR. The temperature comparison (Figure 2) is encouraging: the measured maximum fuel temperature is closely followed by both calculated segment curves. Segment 2 is predicted slightly hotter than the grouped segments 1 and 3, which is consistent with the separate dashed curve and with the expectation that the central segment experiences the most severe thermal conditions in a segmented rod.

The pressure prediction (Figure 2) follows the measured trend initially but begins to diverge in the later part of the irradiation. Up to roughly 7,000 h, the measured and calculated internal pressures remain fairly close, which indicates that the code correctly captures the early gas release and free-volume response. Beyond that point, the measured pressure increases more steeply and reaches nearly 5 MPa, whereas the calculation rises only to about 3.7 MPa. This discrepancy mirrors the divergence in cumulative FGR and supports the conclusion that the gas release model, rather than the thermal model, is responsible for the late underprediction.

The most evident result for IFA-677Rod1 is shown in the bottom panel. The calculated cumulative FGR reaches only about 9%, compared with an experimental value of approximately 22%, and the rapid late-stage rise is only weakly reproduced. The model therefore captures the occurrence of continued release, but not the magnitude or rate of the final increase.

This pattern is consistent with a regime in which intragranular diffusion remains the dominant limiting process in the calculation, whereas the actual rod appears to have entered a higher-release regime influenced by grain-boundary saturation, bubble interconnection, cracking-assisted release, or burnup-driven microstructural evolution [2, 3, 6, 7].

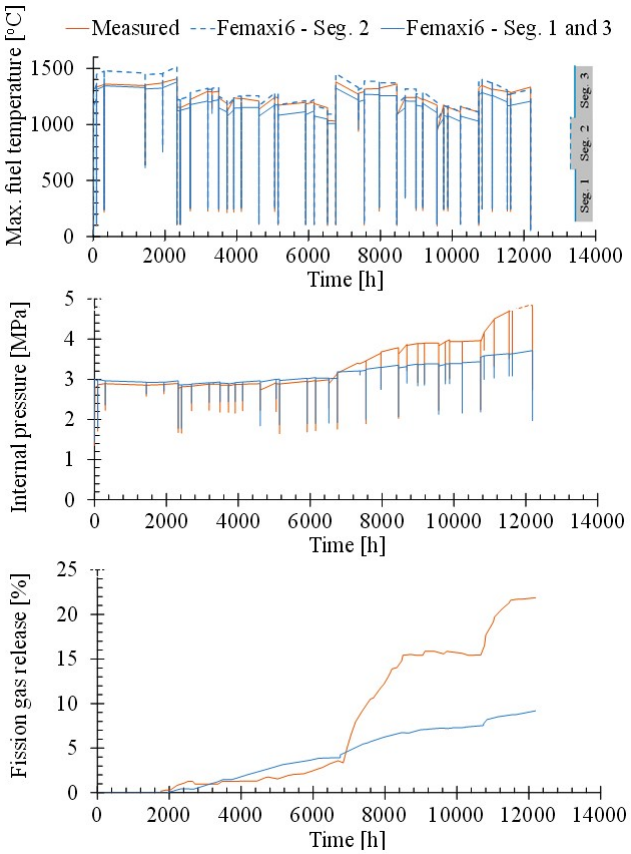


Fig. 2. Comparison of measured and FEMAXI-6 calculated maximum fuel temperature, internal pressure and cumulative FGR for IFA-677Rod1

Experiment IFA-677Rod5

IFA-677Rod5 is a more balanced case (Figure 3). The temperature comparison is again very good, with the measured signal lying between or close to the two calculated segment curves for most of the irradiation. This confirms that the implemented diffusivity is driven by a thermal history that is itself credible. The pressure history also shows good agreement for most of the duration of the experiment, with only a late moderate underprediction: measured pressure rises above approximately 4 MPa while the calculation remains slightly lower.

The FGR comparison is significantly better than for IFA-677Rod1. The model reproduces the onset of release at about the correct time and follows the measured increase reasonably well through the intermediate irradiation period. At end of irradiation, the calculation gives around 11% compared with a measured value about 15–16%. The underprediction remains substantial in absolute terms, but it is no longer severe. This suggests that, for IFA-677Rod5, the corrected diffusivity captures a large fraction of the relevant transport physics, with the remaining gap most likely stems from the boundary-release side of the model rather than from the intragranular diffusivity alone.

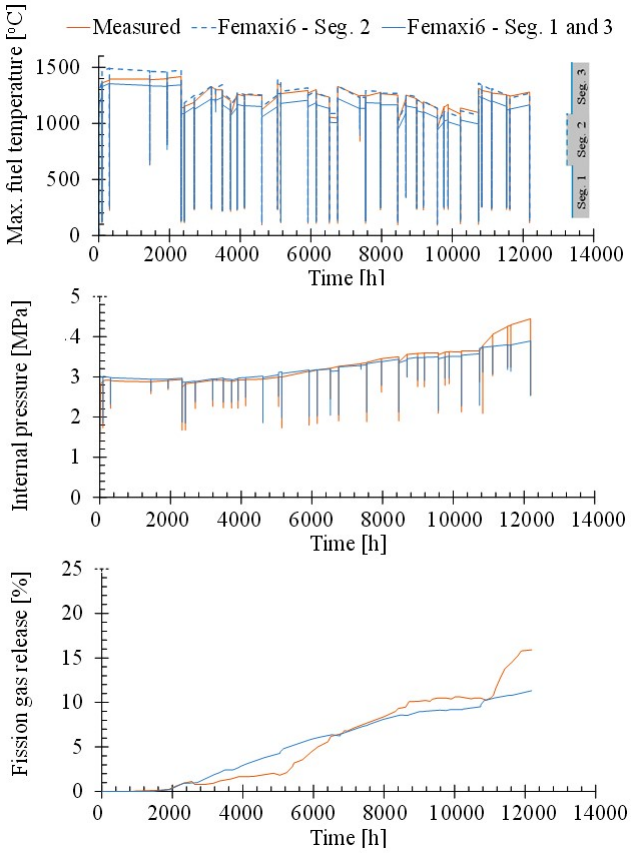


Fig. 3. Comparison of measured and FEMAXI-6 calculated maximum fuel temperature, internal pressure and cumulative FGR for IFA-677Rod5

IFA-677Rod5 is important because it demonstrates that the Cooper-based correction is not just numerically stable; it is also useful. The calculation does not collapse into a too-slow or too-fast release mode, but instead follows the experimental slope for a long portion of the irradiation. This is exactly the behaviour expected from a corrected diffusivity that improves the intragranular gas mobility, while remaining dependent on the pre-existing engineering release framework. It also shows that the difference between rods within the same experiment cannot be interpreted just as a defect of the corrected diffusivity. Case-specific microstructure and local segment conditions are likely to be considered.

Experiment IFA-677Rod6

IFA-677Rod6 (Figure 4) provides an instructive intermediate between the previous two rods. The temperature agreement remains strong, and the calculation captures the overall level and variation of the measured maximum fuel temperature. The pressure prediction is similarly good through most of the irradiation and deviate mainly during the final pressure rise. The correlation between pressure underprediction and FGR underprediction is again evident.

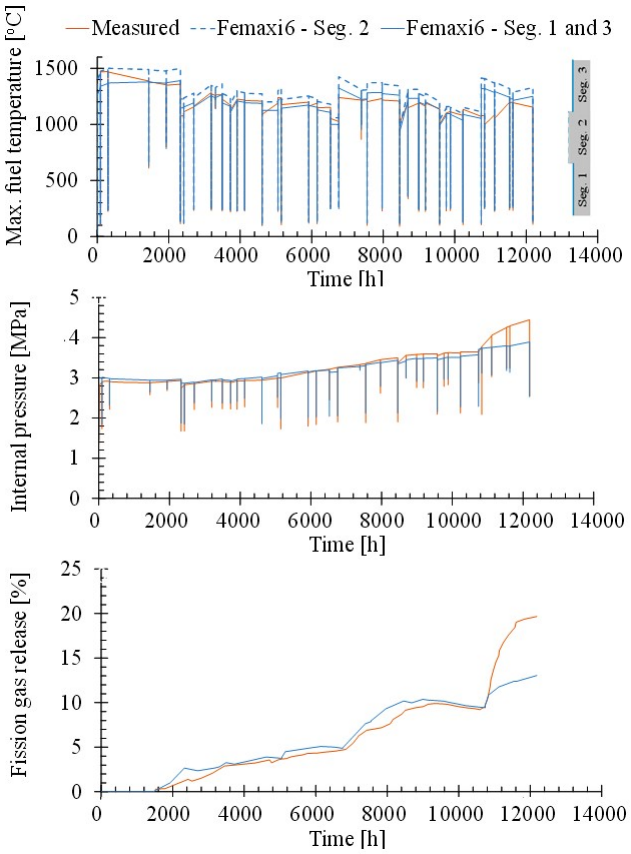


Fig. 4. Comparison of measured and FEMAXI-6 calculated maximum fuel temperature, internal pressure and cumulative FGR for IFA-677Rod6

The FGR curve shows that the calculation initially rises somewhat faster than the measurement and even approaches it by the middle of life. However, as the experiment progresses, the measured release accelerates and reaches 19–20%, while the estimated value saturates around 13%. In other words, the model captures the cumulative character of release but does not sustain the high terminal release rate seen in the experiment. This is a different failure mode from IFA-677Rod1, where even the mid-to-late evolution was too weak; in IFA-677Rod6 the issue is more specifically the inability to maintain the late acceleration.

This behaviour suggests that the corrected diffusivity is already improving the transport part of the problem, but the code still lacks a mechanism that becomes dominant only after a sufficient gas inventory has accumulated at boundaries. Grain-boundary tunnel formation, transient opening of cracked boundaries, or high-burnup porosity connectivity are all viable options [3, 4, 6, 7]. The fact that IFA-677Rod6 is better reproduced than IFA-677Rod1 but still ends too low is consistent with a threshold-type missing mechanism whose activation depends on rod-specific conditions not fully represented in the current model.

ExperimentIFA-716Rod1

IFA-716 is qualitatively different from IFA-677, and IFA-716Rod1 clearly illustrates this (Figure 5). The operating power is lower and the total irradiation time is longer. The measured maximum fuel temperature is reproduced well by the calculated segment curves. Internal pressure is reproduced acceptably in the early and middle periods of irradiation, but the late measured increase above about 3.8 MPa is only partially captured by the calculation.

For FGR, the model predicts a gradual release that starts well before the measured onset. Up to roughly 11,000 h, the experiment indicates basically zero measured release while the calculation has already accumulated a few percent. However, once the measured release begins, the experimental curve rises rapidly and nearly catches up to the calculation. The final values are actually rather similar, around 5.6% measured versus about 5.1% calculated. This is an important result: despite the incorrect timing of onset, the overall end-of-life release is predicted with high confidence.

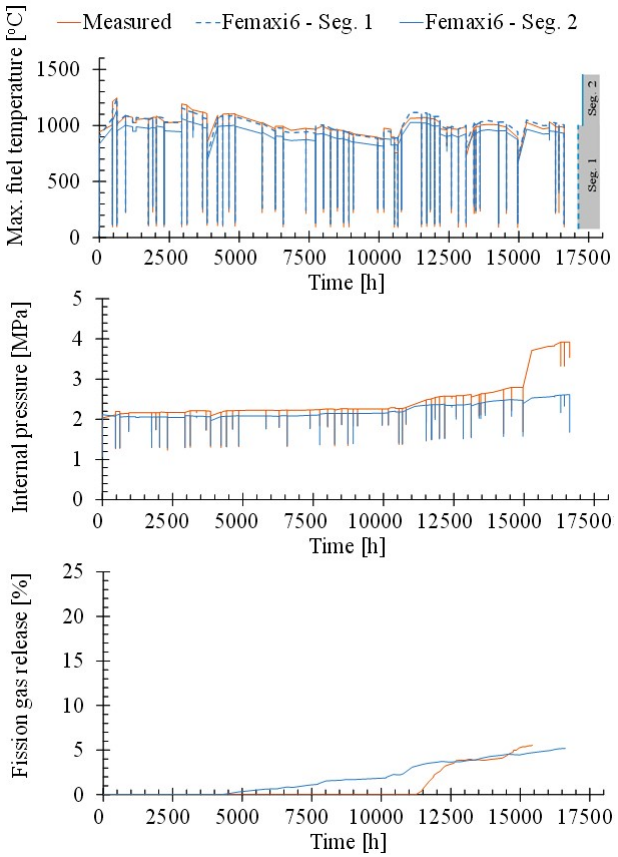


Fig. 5. Comparison of measured and FEMAXI-6 calculated maximum fuel temperature, internal pressure and cumulative FGR for IFA-716Rod1

The results suggest that, for IFA-716Rod1, the corrected diffusivity may already provide an adequate description of the total integrated transport, while the closure used to determine when grain-boundary gas is counted as released is not fully consistent with the experiment. In a rod with low absolute release, a minor difference in the release threshold can produce an apparently large shift in onset time without significantly affecting the final integral value. IFA-716Rod1 should therefore not be taken as a simple model failure, but rather as evidence that improved release initiation treatment and segment-specific measurement interpretation may be required.

ExperimentIFA-716Rod6

IFA-716Rod6 is the best overall case in the assessment set (Figure 6). Temperature agreement is again strong, and the internal pressure curve is reproduced with only small deviations over most of the irradiation. The late pressure level is slightly underpredicted, but the difference remains modest compared with the higher-release of IFA-677rods.

The FGR comparison reveals a similar pattern to IFA-716Rod1, but with better overall consistency. The calculation predicts a gradual accumulation of released gas prior to the measured onset, which implies that the model is somewhat too permissive in the low-release regime. However, once measured release begins, the two curves remain close and end with only a slight difference, about 6.2% calculated versus 6.8% measured. The slope following onset is also reproduced satisfactorily.

The good performance for IFA-716Rod6 is instructive because it defines the regime in which the present implementation is already adequate for engineering use: moderate release, well-predicted temperatures, and no strong terminal acceleration beyond what the corrected diffusivity can represent. In that regime, the Cooper correction incorporated in FEMAXI-6 appears capable of providing a realistic integrated FGR estimate without further changes to the surrounding release framework.

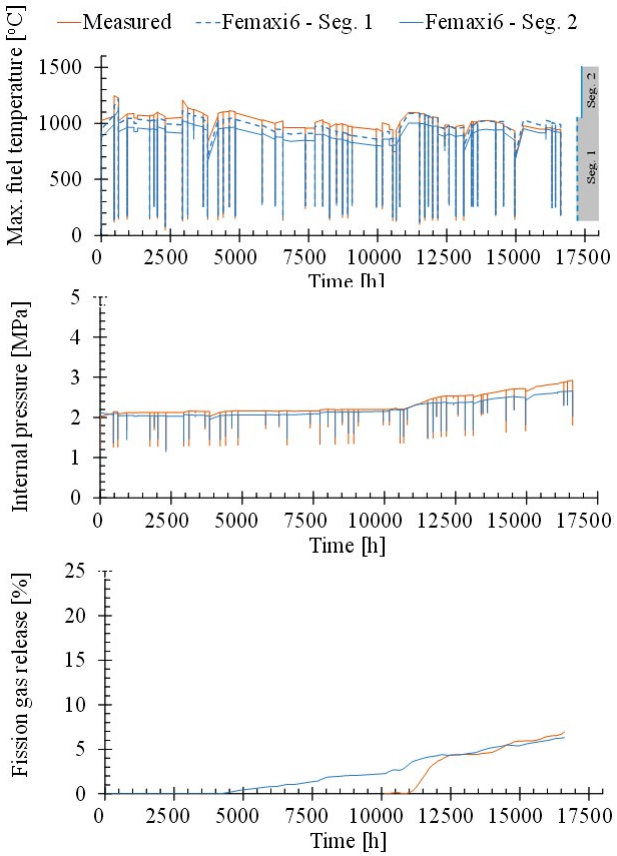


Fig. 6. Comparison of measured and FEMAXI-6 calculated maximum fuel temperature, internal pressure and cumulative FGR for IFA-716Rod6

Limitations of the present study

The present study has three explicit limitations. First, the quantitative final FGR values were read approximately from the figures [9-11] because raw numerical benchmark tables were not available in the provided material. Second, since the study focuses on a targeted implementation, the FEMAXI-6 gas release framework is not re-tuned. Third, the work evaluates Cooper case A, and the other alternative Cooper parameterization (case B) [8] was not investigated here. These limitations do not invalidate the conclusions, but they should be taking into account when assessing the precise extent of the reported errors.

Conclusions

A corrected fission-gas diffusivity based on the Cooper case A formulation was successfully implemented in FEMAXI-6. This involved replacing the standard undoped fuel effective diffusivity with a temperature-dependent correction applied to the D_1 and D_2 components while preserving D_3.

The implemented model is numerically stable and preserves the FEMAXI-6 standard engineering workflow.

Across the five analyzed rods, the model accurately reproduces the maximum fuel temperature and captures the overall pressure trend, demonstrating that the corrected diffusivity is functioning within a credible thermo-mechanical solution.

For cumulative FGR, the model performs well for the moderate-release of rods IFA-716Rod1 and IFA-716Rod6, and gives partial improvement for IFA-677Rod5 and IFA-677Rod6, but it strongly underestimates the high late release of IFA-677Rod1.

The primary remaining deficiency is not the absence of thermal sensitivity, but the lack of a sufficiently strong late-stage release mechanism associated with grain-boundary saturation, cracking-assisted release, or burnup-driven microstructural evolution.

The most defensible path forward is therefore to retain the current Cooper-corrected diffusivity and supplement it with an improved grain-boundary release model, rather than replacing it with another purely effective diffusivity correlation.

References

[1] Booth, A.H. (1957) ″A method of calculating the fraction of rare gas fission products that diffuses out of a UO_2 fuel element under reactor conditions″, Atomic Energy of Canada Limited, *CRCD-721 Report*, Canada.

[2] Matzke, H. (1980) ″Gas release mechanisms in UO_2 - a critical review″, *Radiation Effects*, Vol. 53, pp. 219–242

[3] Rest, J., Cooper, M.W.D., Spino, J., Turnbull, J.A., Van Uffelen, P., Walker, C.T. (2019) ″Fission gas release from UO_2 nuclear fuel: a review″, *Journal of Nuclear Materials*, Vol. 513, pp.310–345.

[4] White, R.J., Tucker, M.O. (1983) ″A new fission-gas release model″, *J. of Nuclear Materials*, Vol. 118, pp. 1–38.

[5] Turnbull, J.A., Friskney, C.A., Findlay, J.R., Johnson, F.A. (1982) ″The diffusion coefficients of gaseous and volatile species during the irradiation of uranium dioxide″, *Journal of Nuclear Materials*, Vol. 107, pp.168–184.

[6] Pastore, G., Pizzocri, D., Hales, J.D., Novascone, S.R., Spencer, B.W., Luzzi, L., Van Uffelen, P., Williamson, R.L. (2018) ″Modelling of transient fission gas behaviour in oxide fuel and application to the BISON code″, *Nuclear Engineering and Design*, Vol. 330, pp. 553–567.

[7] Barani, T., Bruschi, E., Pizzocri, D., Pastore, G., Van Uffelen, P., Luzzi, L., Williamson, R.L. (2017) ″Analysis of transient fission gas behaviour in oxide fuel using BISON and TRANSURANUS″, *J. of Nuclear Materials*, Vol. 486, pp. 96–110.

[8] Cooper, M.W.D., Pastore, G., Che, Y., Matthews, C., Forslund, A., Stanek, C.R., Shirvan, K., Tverberg, T., Gamble, K.A., Mays, B., Andersson, D.A. (2020) ″Fission gas diffusion and release for Cr_2O_3-doped UO_2: from the atomic to the engineering scale″, *Journal of Nuclear Materials*, Vol. 545, paper ID 152590.

[9] Che, Y. (2022) *″Application of data-driven methods in nuclear fuel performance analysis″*, Thesis, Massachusetts Institute of technology, USA.

[10] Gamble, K.A., Pastore, G., Andersson, D., Cooper, M.W.D. (2019) ″ATF material model development and validation for priority fuel concepts″, INL-EXT--19-54769-Rev000 report, Idaho National Laboratory, USA, https://doi.org/10.2172/1547325

[11] Toptan, A., Angulo Barba, F., Che, Y., Gamble, K.A., Singh, G., Galvin. C.O.T, Cooper, M.W.D. (2022) ″BISON Capability to Account for Dopant Sensitivity in Relevant UO_2 Material Models″, Office of Scientific and Technical Information, *Technical Report OSTI ID 1891508*, US Depart. of Energy, https://doi.org/10.2171.1891508

[12] Nakajima, T., Saito, H., Osaka, T. (1994) ″FEMAXI-6-IV: a computer code for the analysis of thermal and mechanical behavior of light water reactor fuel rods″, *Nuclear Engineering and Design*, Vol. 148, pp. 41–52.